ELSEVIER

Thermochimica Acta 330 (1999) 75–83

thermochimica acta

Computer simulation of the melting kinetics of polymer crystals under condition of modulated temperature[1]

Akihiko Toda*, Takeshi Arita, Chiyoko Tomita, Masamichi Hikosaka

Faculty of Integrated Arts and Sciences, Hiroshima University, 1-7-1 Kagamiyama, Higashi-Hiroshima 739-8521, Japan

Received 12 August 1998; accepted 11 January 1999

Abstract

Computer simulation has been applied to the modeling of the melting kinetics of polymer crystals, which we have recently presented to predict the response of the kinetics to a sinusoidal modulation in temperature on heating. The frequency and heating-rate dependencies have been examined with a Gaussian or uniform distribution of the melting points. For both of the distributions, the details of the dependence have been examined on the basis of the analytical results of the modeling. It has also been confirmed that the response of the kinetics has higher harmonics as expected from the formulation of the modeling. This behavior corresponds to the experimental results of temperature-modulated DSC (T-MDSC) in the melting region of polymer crystals. © 1999 Elsevier Science B.V. All rights reserved.

Keywords: Temperature-modulated DSC; Kinetics of melting; Polymer crystals; Computer simulation

1. Introduction

In a temperature-modulated differential scanning calorimetry (T-MDSC) [1–6], we apply a temperature modulation to the sample temperature, T_s, under linear heating/cooling or isothermal condition. We obtain a response in the modulated heat flow, $\dot{Q}$, which is related to the modulation in sample temperature with an apparent heat capacity, $\Delta\tilde{C}\,e^{-i\alpha}$, defined as

$$T_s = \bar{T}_s + \tilde{T}_s\,e^{i(\omega t+\epsilon)}, \tag{1}$$

$$\dot{Q} = \bar{\dot{Q}} + \tilde{\dot{Q}}\,e^{i(\omega t+\delta)}, \tag{2}$$

$$\tilde{\dot{Q}}\,e^{i(\omega t+\delta)} = -\Delta\tilde{C}\,e^{-i\alpha}\frac{d}{dt}\tilde{T}_s\,e^{i(\omega t+\epsilon)}, \tag{3}$$

$$\Delta\tilde{C}\,e^{-i\alpha} \equiv \Delta\tilde{C}' - i\Delta\tilde{C}'', \tag{4}$$

where $\bar{T}_s$ can be linear heating or cooling, $\bar{T}_s=\beta t$, or a constant temperature.

The apparent heat capacity is a complex quantity in the temperature range of a relaxation process such as the α process related to the glass transition [7–9] and in the range of phase transitions such as crystallization [10–14] and melting [1–3,15–18]. In the melting region of polymer crystals, it is known that the apparent heat capacity shows large peaks in magnitude and phase angle. We have argued that the response of the melting kinetics is responsible for these large changes [16–18].

In the present paper, we examine the response of the melting kinetics of polymer crystals through a computer simulation based on our modeling of the process.

*Corresponding author. Tel.: +81-824-24-6558; fax: +81-824-24-0757; e-mail: atoda@ipc.hiroshima-u.ac.jp

[1]Presented in part at the Fifth Lähnwitz Seminar on Calorimetry, Külungsborn, Germany, 7–12 June 1998.

PII: S0040-6031(99)00021-0

In the following, we first review the basic idea of our approach and then show the analytical results of the modeling. The method of computer simulation is presented subsequently and the results are examined on the basis of the analytical results.

2. Modeling [16,17]

2.1. A basic model

In the transformation region, the heat flow to and from the sample can be represented by the sum of the contribution from heat capacity and of the exo- or endothermic heat flow of transformation, $F(t)$:

$$\dot{Q} = -mc_p \frac{\mathrm{d}T_\mathrm{s}}{\mathrm{d}t} + F(t). \tag{5}$$

Since the rate of transformation is a function of supercooling or superheating and hence of T_s, the heat flow can be expanded about the sample temperature for sufficiently small modulation [1–3,19]:

$$F(t, T_\mathrm{s}) = \bar{F}(t, \bar{T}_\mathrm{s}) + F'_T(t, \bar{T}_\mathrm{s})\tilde{T}_\mathrm{s}\,\mathrm{e}^{\mathrm{i}(\omega t+\epsilon)} + \cdots. \tag{6}$$

The second term in the expansion must be in balance with the modulation components of heat flow and of contribution of heat capacity:

$$\tilde{\dot{Q}}\,\mathrm{e}^{\mathrm{i}(\omega t+\delta)} = -mc_p \frac{\mathrm{d}}{\mathrm{d}t}\tilde{T}_\mathrm{s}\,\mathrm{e}^{\mathrm{i}(\omega t+\epsilon)} + F'_T\tilde{T}_\mathrm{s}\,\mathrm{e}^{\mathrm{i}(\omega t+\epsilon)}. \tag{7}$$

By re-arranging the relationship, we obtain the expression of the apparent heat capacity in the transformation region:

$$\Delta\tilde{C}\,\mathrm{e}^{-\mathrm{i}\alpha} = mc_p + \frac{\mathrm{i}}{\omega}F'_T. \tag{8}$$

This is the expression of the apparent heat capacity on which our modeling of the melting kinetics is based.

2.2. Melting of polymer crystals

Polymer samples are aggregates of small crystallites, the melting points of which have a continuous distribution mainly determined by the distribution of lamellar thickness of crystals and the distribution of molecular weight of polymer chains. The wide distribution of melting points is responsible for the broad endothermic peak (e.g. $\geq$20 K) in the melting region of polymer crystals [20]. Hence, we need to consider the successive melting of the crystallites in the melting region for a heating run.

We consider the melting process of the crystallites by introducing the crystallinity of a fraction, $\phi(t, T_\mathrm{m})$, having the melting point in the range from T_m to $T_\mathrm{m}+\mathrm{d}T_\mathrm{m}$. Then, we employ the simplest kinetics of melting by utilizing the following differential equation:

$$\frac{\mathrm{d}}{\mathrm{d}t}\phi(t, T_\mathrm{m}) = -R(\Delta T)\phi(t, T_\mathrm{m}), \tag{9}$$

where R represents the coefficient of the total melting rate and is determined by the superheating $\Delta T \equiv T_\mathrm{s} - T_\mathrm{m}$.

We further assume that the heating run satisfies the condition of heating only ($\mathrm{d}T_\mathrm{s}/\mathrm{d}t > 0$), and hence we do not have to consider the reverse process of crystallization; the process therefore becomes a one-way transformation of melting and the interpretation will be straightforward. Then, the solution of Eq. (9) is simply given as

$$\phi(t, T_\mathrm{m}) = \phi(0, T_\mathrm{m}) \exp\left[-\int_0^t R\,\mathrm{d}t'\right]. \tag{10}$$

The total crystallinity, $M_\mathrm{c}(t)$, and the endothermic heat flow of melting, $F_\mathrm{melt}(t)$, are expressed by the fractions as

$$M_\mathrm{c}(t) = \int_0^\infty \mathrm{d}T_\mathrm{m}\,\phi(t, T_\mathrm{m}), \tag{11}$$

$$F_\mathrm{melt}(t) = \Delta H \frac{\mathrm{d}M_\mathrm{c}}{\mathrm{d}t}, \tag{12}$$

where $\Delta H(>0)$ represents the enthalpy change of the system on melting.

It is noted that in the present treatment we will not consider the contribution of re-crystallization and re-organization in the melting region, because we expect much smaller response of those processes to temperature modulation than that of melting as is the case for crystallization [16–18].

2.3. Assumption of a uniform distribution of the melting points

In order to obtain the analytical expression of the response of heat flow to temperature modulation, we need to assume a steady state and the same form of $R(\Delta T)$ for the fractions. The steady state is realized with a uniform distribution of the fractions at the initial state:

$$\phi(0, T_m) = \phi_0. \tag{13}$$

For the uniform distribution, the steady response in heat flow to a sinusoidal modulation of temperature should be represented by a Fourier series expressed as

$$F_{melt}(t) = \bar{F}_{melt} + F'_T(\omega)\tilde{T}_s\, e^{i\omega t} + \tfrac{1}{2}F''_T(\omega)\tilde{T}_s^2\, e^{2i\omega t} + \cdots, \tag{14}$$

$$\bar{F}_{melt} = -\Delta H\phi_0\beta, \tag{15}$$

$$F'_T(\omega)\tilde{T}_s = \phi_0\beta\int_{-\infty}^{\infty} dt\, e^{-i\omega t} F_{melt}(t). \tag{16}$$

The contribution of the melting kinetics to the apparent heat capacity, f, is then defined as

$$\Delta\tilde{C}\, e^{-i\alpha} = mc_p + f(\omega), \tag{17}$$

$$f(\omega) \equiv f\, e^{-i\gamma} = f'(\omega) - if''(\omega) = \frac{i}{\omega}F'_T(\omega). \tag{18}$$

2.4. R_0, R_1 and R_e

We have analytically examined the following three different dependencies on superheating of the melting rate coefficient. As shown below, the melting kinetics is described by a characteristic time, τ, which is dependent on the heating rate, β, as $\tau \propto \beta^x$ with $-1 \le x \le 0$.

(i) *Melting rate independent of superheating:*

$$R_0: \text{ independent of } \Delta T, \tag{19}$$

$$\phi_0(\Delta t) = \phi_0 \exp\left(-\frac{\Delta t}{\tau_0}\right), \tag{20}$$

$$f_0(\omega) = \frac{\Delta H\phi_0}{1 + i\omega\tau_0}, \tag{21}$$

$$\tau_0 \equiv \frac{1}{R_0}. \tag{22}$$

(ii) *Linear dependence of the melting rate on superheating:*

$$R_1 = a\Delta T, \tag{23}$$

$$\phi_1(\Delta t) = \phi_0 \exp\left(-\left(\frac{\Delta t}{2\tau_1}\right)^2\right), \tag{24}$$

$$f_1(\omega) = \frac{\Delta H\phi_0}{\omega\tau_1}\left\{ e^{-(\omega\tau_1)^2}\int_0^{\omega\tau_1} e^{x^2}\, dx - i\frac{\sqrt{\pi}}{2}\left(1 - e^{-(\omega\tau_1)^2}\right)\right\}, \tag{25}$$

$$\tau_1 \equiv \left(\frac{1}{2a\beta}\right)^{1/2}. \tag{26}$$

(iii) *Exponential dependence of the melting rate on superheating:*

$$R_e = \frac{a}{c}(e^{c\Delta T} - 1), \tag{27}$$

$$f_e(\omega) = \frac{\Delta H\phi_0}{1 + \omega\tau_e}\frac{1}{\tau'_e}\int_0^{\infty} dx\,(e^{x/\tau_e} - e^{-i\omega x}) \times \exp\left[-\frac{\tau_e}{\tau'_e}\left(e^{x/\tau_e} - 1 - \frac{x}{\tau_e}\right)\right], \tag{28}$$

$$\tau_e \equiv \frac{1}{\beta c}, \tag{29}$$

$$\tau'_e \equiv \frac{c}{a}. \tag{30}$$

(a) For $\tau_e/\tau_e' \gg 1$, $R_e \simeq R_1$, $\phi_e \simeq \phi_1$ and $f_e \simeq f_1$ with $\tau_1 = (\tau_e\tau'_e/2)^{1/2}$.

(b) For $\tau_e/\tau_e' \ll 1$,

$$R_e \simeq \frac{a}{c}e^{c\beta\Delta t}, \tag{31}$$

$$\phi_e(\Delta t): \text{ nearly stepwise at } \Delta t \sim \tau_e, \tag{32}$$

$$f_e(\omega) \simeq \frac{\Delta H\phi_0}{1 + i\omega\tau_e}. \tag{33}$$

3. Method of computer simulation

We consider the distribution of melting points of the following forms corresponding to the actual distribution and to the uniform distribution of the melting

points:

$$\phi_0(T_m^k) \propto \exp\left[-\frac{1}{2}\left(\frac{k-\bar{M}}{\sigma}\right)^2\right], \tag{34}$$

$$\phi_0(T_m^k): \text{ constant}, \tag{35}$$

$$T_m^k \equiv \beta\Delta t k, \tag{36}$$

where T_m^k is taken discretely with the temperature change, $\beta\Delta t$, in a unit time, Δt. In Eq. (34), $\bar{M}$ and σ are the mean temperature and the peak width of the distribution, respectively, normalized by $\beta\Delta t$; typical values of them were 5000 and 1000 for 10 000 sites of T_m^k.

Sample temperature and the melting kinetics are considered by the discrete time change, Δt, as follows:

$$T_s(j\Delta t) = \beta j\Delta t + \tilde{T}_s \sin(\omega j\Delta t), \tag{37}$$

$$\Delta\phi^k((j+1)\Delta t) \equiv \phi((j+1)\Delta t, T_m^k) - \phi(j\,\Delta t, T_m^k) = -R(\Delta T)\phi(j\Delta t, T_m^k)\Delta t, \tag{38}$$

$$F_{melt}(j\,\Delta t) = -mc_p[\beta + \tilde{T}_s\omega\cos(\omega j\Delta t)] + \Delta H\sum_k \frac{\Delta\phi^k(j\Delta t)}{\Delta t}, \tag{39}$$

where mc_p in Eq. (39) is the true heat capacity assumed to be constant (or zero) in the following. The unit time Δt (<0.2 s) was properly selected for the applied modulation period taken from 1 to 800 s. The heating rate of β=1 K min^{-1} was mainly examined in the simulation.

In order to incorporate the condition out of heating only, it is assumed that the melting-rate coefficient becomes zero for ΔT<0. This condition is based on the fact that the superheating and supercooling dependence of melting and crystallization rates, respectively, is quite asymmetric [20]; namely, crystallization needs a much larger ΔT.

In the case of uniform distribution of the melting points, we ran the simulation at least over 10 times the modulation period to confirm the steady state of the process. The obtained heat flow and the modulated sample temperature were then analyzed by the same procedure as the experimental data [5].

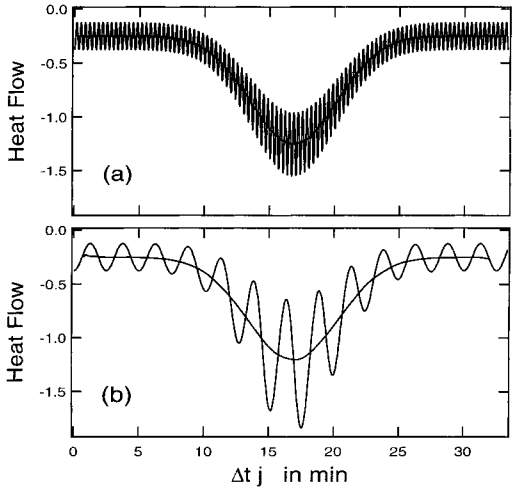

Fig. 1. Raw data of heat flow for different modulation periods of (a) 20 and (b) 150 s. The parameters are the following: Δt=0.2 s, β=1 K min^{-1}, $\omega\tilde{T}_s/\beta$=0.5, R=0.74ΔT and $mc_p/\Delta H\phi_0^{max}$=1/4.

4. Results

4.1. Gaussian distribution of melting points

Fig. 1 shows the raw data of the heat flow with R_1=$a\Delta T$ for different modulation periods and Fig. 2 shows the frequency response of the apparent heat capacity determined from the raw data. In Fig. 3, the

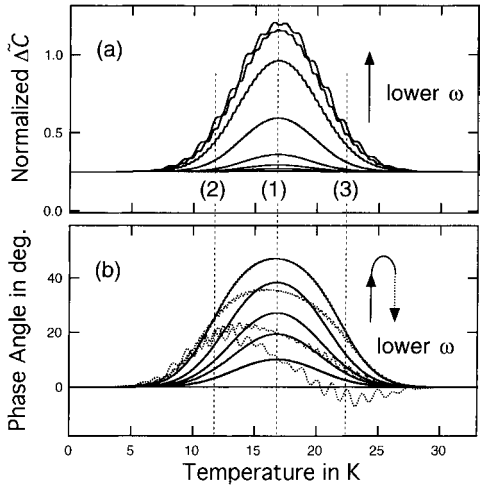

Fig. 2. Apparent heat capacity determined from the raw data as typically shown in Fig. 1. Modulation periods are 2, 4, 6, 10, 20, 40, 80, and 150 s.

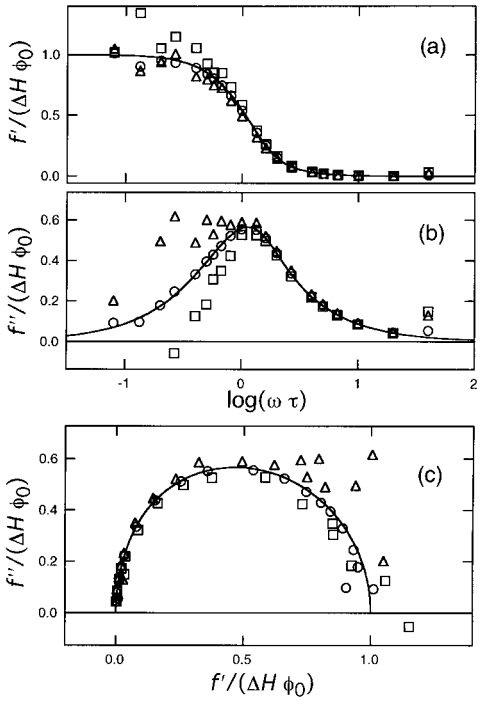

Fig. 3. Frequency dependence of the contribution of melting kinetics, $f(\omega)$, examined at three different temperatures marked in Fig. 2 as (1) ○, (2) △, (3) □. The fitting lines represent the analytical solution of Eq. (25) for R_1.

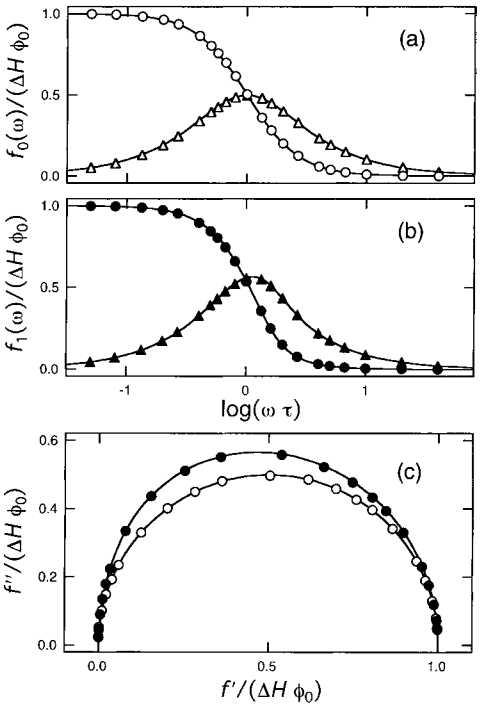

Fig. 4. Results of computer simulation (○, △, ●, ▲) compared with the analytical solutions (lines) of Eqs. (21) and (25) for (a) R_0 and (b) R_1, respectively. Symbols (○, ●) and (△, ▲) in (a) and (b) represent real and imaginary components, respectively. In the Cole–Cole plot of (c), symbols ○ and ● correspond to the cases of R_0 and R_1, respectively. The parameters are as follows: β=1 K min^{-1}, $\omega\bar{T}_s/\beta$=0.5 and (a) R_0=0.157 and (b) R_1=0.74ΔT.

dependence is examined at three different temperatures marked in Fig. 2. The basic feature in Fig. 3 is well described by the analytical solution of Eq. (25) for R_1 and is similar to the behavior observed experimentally [16–18]. For (2) and (3) in the shoulder of the peak in Fig. 2, the dependence shown in Fig. 3 deviates from the fitting curve for shorter ω (longer modulation period). This behavior should be due to the change in the distribution of melting points on both sides of the peak, and hence it must be due to the condition of loss of steady state; we can also observe a similar behavior experimentally [16–18].

4.2. Uniform distribution of melting points

Figs. 4 and 5 show the results of computer simulation compared with the numerical calculations of the analytical solutions of Eqs. (21), (25) and (28) for R_0, R_1 and R_e, respectively. The agreement between simulation and numerical calculation is quite satisfactory. As is seen in Fig. 4, the difference in the frequency dependence of f_0 and f_1 is not large, and hence we may be allowed to fit the data with a frequency response function of Debye's type equivalent to f_0.

In Fig. 6, the heating condition is examined for $\omega\tau$=1. The simulation results of $f(\omega)$ are in good agreement with the analytical results if the condition is heating only, which is expressed as $\omega\bar{T}_s/\beta < 1$ from Eq. (1). In the analytical treatment, we have assumed the heating-only condition. When the condition is not satisfied, the melting process stops for some fraction of time (R=0 for ΔT<0) in the range dT_s/dt<0 and hence the magnitude of the response decreases (Fig. 6(a)); the same effect will be responsible for the change in the phase angle in Fig. 6(b).

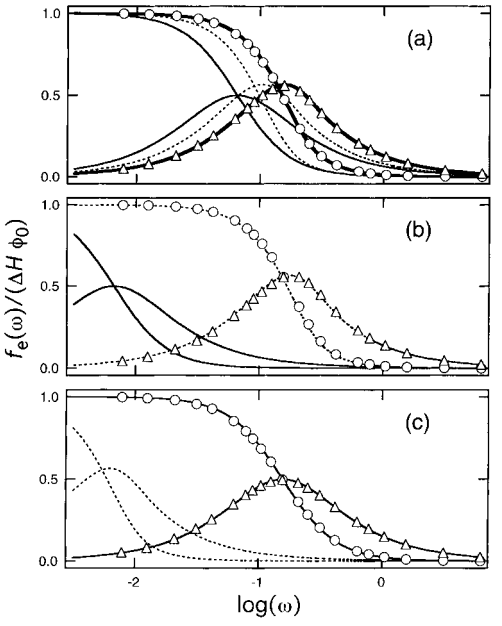

Fig. 5. Results of computer simulation (○, △) compared with the analytical solution (thick line) of Eq. (28) for R_e. The thin and dotted lines represent $f(\omega)$ of Eqs. (33) and (25) with $\tau_1=(\tau_e\tau_e'/2)^{1/2}$, respectively. Symbols ○ and △ represent real and imaginary components, respectively. In (a), $\tau_e/\tau_e'=1$ and the asymptotic behaviors are confirmed for $\tau_e/\tau_e'\gg1$ and $\ll1$ in (b) and (c), respectively. The parameters are the following: β=1 K min^{-1}, $\omega\tilde{T}_s/\beta$=0.5 and τ_e/τ_e'= (a) 15.34/15.34, (b) 150.1/0.540 and (c) 6.37/10 000 s/s.

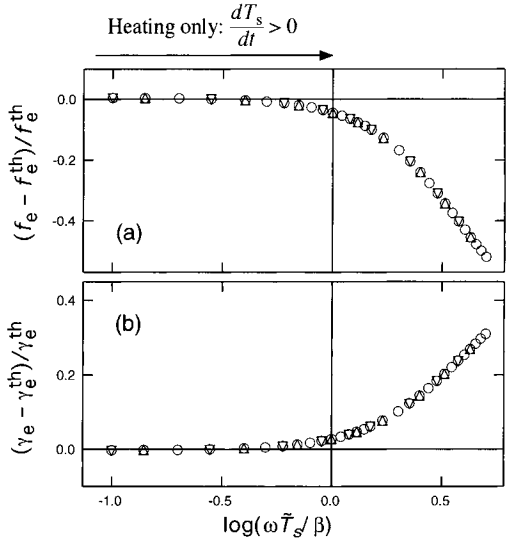

Fig. 6. Comparison of the simulation results of $f_e\,e^{-i\gamma_e}$ defined in Eq. (18) with the analytical solution of $f_e^{th}\,e^{-i\gamma_e^{th}}$ for R_e ($\tau_e/\tau_e'\ll1$) in Eq. (33) for different heating conditions (the variable was $\tilde{T}_s$). Different symbols correspond to (period in s, β in K min^{-1})=(○) (40, 1), (△) (40, 2) and (▽) (20, 1). Melting-rate coefficient of R_e has been employed with the coefficients of a and c adjusted to satisfy $\omega\tau=1$: (a in K^{-1} s^{-1}, c in K^{-1})=(○) (0.000942, 9.42), (△) (0.000471, 4.71) and (▽) (0.00188, 18.8). The range of $\omega\tilde{T}_s/\beta<1$ corresponds to heating only ($dT_s/dt>0$).

4.3. Heating-rate dependence of the characteristic time

From a dimensional analysis, it is expected that the heating-rate dependence of the characteristic time, τ, is determined by the superheating dependence of the melting-rate coefficient, R, as follows:

$$R(\Delta T) \propto \Delta T^{y}, \tag{40}$$

$$\tau(\beta) \propto \beta^{-y/(y+1)}, \tag{41}$$

which agrees with the results of the analysis shown in Eqs. (22), (26) and (29); in the case $R_e \propto e^{c\Delta T}$, $y \to \infty$.

By examining the frequency dependence of the apparent heat capacity for the uniform distribution of the melting points, we have obtained the characteristic time, τ, from the peak frequency ($\omega\tau=1$) which gives a maximum in f''. We have done the analysis with different heating rate and determined the exponent of the heating-rate dependence of the characteristic time. We examined the cases of R_0: independent of ΔT, $R_{1/2}\propto\Delta T^{1/2}$, $R_1\propto\Delta T$, $R_2\propto\Delta T^2$ and $R_e\propto e^{c\Delta T}$ and confirmed the above relationship between $R(\Delta T)$ and $\tau(\beta)$.

4.4. Non-linear response

The kinetic model which we have employed (Eqs. (19)–(22) and Eqs. (34)–(39)) does not assume linear response and hence the results of the computer simulation show non-linearity. The non-linear response can be easily recognized by the plots of Lissajous diagram in Fig. 7(a)–(c). For R_0 in Fig. 7(a), the diagram is a circle because the response is linear as will be discussed below. For R_1 and R_e, the deformation of the circle is clearly seen in Fig. 7(b) and (c), respectively.

The non-linear behavior is also seen in the plot of the ratio of the second harmonic to the first harmonic

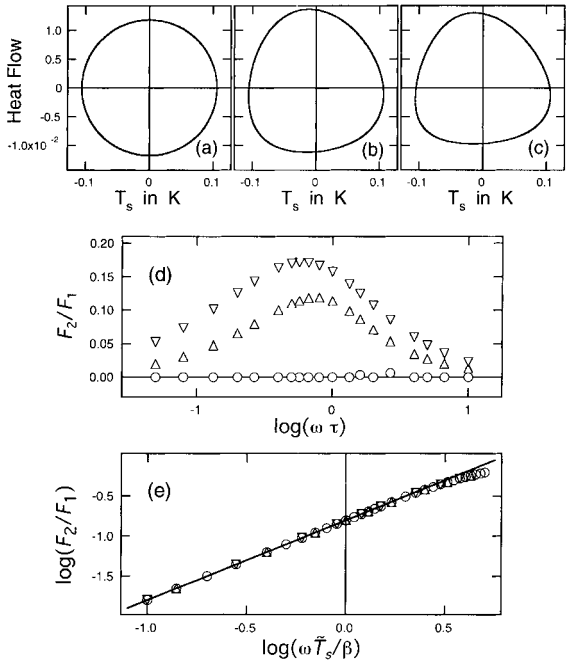

Fig. 7. Nonlinear response shown in Lissajous diagrams, (a)–(c), and in the plots of the ratio of the second harmonic, F_2, to the first harmonic, F_1, of modulated heat flow, (d) and (e). In the Lissajous diagrams (a)–(c) and in (d), the melting-rate coefficient is R_0 (a and ○), R_1 (b and △) and R_e (c and ▽): R_0=0.1571, R_1=0.740ΔT and R_e=10^{-4}($e^{9.425\Delta T}$−1). In (a)–(c), the modulation period was 40 s. Other parameters for (a)–(d) are β=1 K min^{-1} and $\omega\tilde{T}_s/\beta$=1. In (e), melting-rate coefficient of R_e has been employed with the same values of the parameter as in Fig. 6. The meanings of the symbols in (e) are also the same as in Fig. 6. The slope of the fitting line in (e) is 1.0.

of modulated heat flow, F_2/F_1, shown in Fig. 7(d). Here again, the response for R_0 is linear (F_2=0), while the others show maximum non-linearity near $\omega\tau$=1 in both cases. It is further conformed in Fig. 7(e) that the ratio, F_2/F_1, increases linearly with $\tilde{T}_s$ because $F_1 \propto \tilde{T}_s$ and $F_2 \propto \tilde{T}_s^2$ as expected in Eq. (14).

5. Discussion

In this paper, we have applied the method of computer simulation to the modeling of the melting kinetics of polymer crystals. We first examined the case of a Gaussian distribution of melting points and confirmed that the frequency dependence of the apparent heat capacity at a given temperature is well described by the corresponding analytical solution which was originally obtained for a uniform distribution of the melting points. In the range where the change in the melting distribution is large, the dependence is modified because one loses steady state. We have previously presented the condition required for the (quasi-)steady state in the following manner [17]:

$$\text{(Temperature range in which the change in } \phi_0(T_m) \text{ is negligible)} \gg \beta \times \text{(period of modulation) and } \gg 2\pi\beta\tau.$$

In the shoulder of the melting peak, the change in $\phi_0(T_m)$ becomes large and the above condition is not satisfied. In the experimental results, we also see similar behavior [16–18].

Second, we examined the behavior with a uniform distribution of melting points with which we can be assured of steady state. The obtained results were in good agreement with the analytical results if the condition of heating only (dT_s/dt>0) is satisfied. Experimentally, we have also confirmed that the apparent heat capacity in the melting range keeps a constant value for dT_s/dt>0 but shows a systematic decrease if the condition is not satisfied [17]. The main reason for the decrease is the supercooling of some fractions during the melting process in the range dT_s/dt<0. Therefore, the condition of heating only provides a simpler situation for the analysis of the melting kinetics.

In the third part of this work, we have confirmed the relationship between the superheating dependence of the melting-rate coefficient, $R(\Delta T)$, and the heating-rate dependence of the characteristic time, $\tau(\beta)$. The modeling of the melting kinetics with R depending on superheating is essential for the dependence of $\tau(\beta)$. If we simply apply the superposition of a relaxation function of $\exp(-t/\tau)$ to obtain the frequency response function of Debye's type, the heating-rate dependence of τ will not be explained. Experimentally [16–18], the dependence of the characteristic time was in the range $-1 \le x \le 0$ with the expression $\tau \propto \beta^x$, and hence it is within the range of the predicted exponent shown in Eq. (41).

In the last part, we examined the non-linear response of the kinetics. For R_0, the response was linear, while the response for R_1 and R_e exhibited non-linearity. The differences can be understood in terms

of the temperature derivative of the melting-rate coefficient. As is typically shown in the following equations which apply to the crystallites having their melting temperature at $T_m=\beta t_0$ with the sample temperature of $T_s = \beta t + \tilde{T}_s \sin[\omega(t - t_0)]$, the expansions of the melting-rate coefficient, R, and the crystallinity, ϕ, at time $t=t_0+\Delta t$ are determined by the temperature derivative of R:

$$R \sim R(\beta\Delta t) + R'(\beta\Delta/t)\tilde{T}_s \sin(\omega\Delta t) + \frac{1}{2}R''(\beta\Delta t)\tilde{T}_s^2 \sin(2\omega\Delta t) + \cdots, \quad (42)$$

$$\phi \sim \phi_0 \, e^{-\int_0^{\Delta t} dx\, R(\beta x)} \left[1 - \tilde{T}_s \int_0^{\Delta t} R'(\beta x) \sin(\omega x)\, dx + \frac{1}{2}\tilde{T}_s^2 \int_0^{\Delta t} R''(\beta x) \sin(2\omega x)\, dx + \cdots \right]. \quad (43)$$

From Eqs. (11) and (12), the heat flow of melting is given by the product of $R\phi$ as

$$F_{melt}(t) = -\Delta H \int_0^{\infty} R\phi \, dT_m. \quad (44)$$

For the constant rate of R_0, the temperature derivatives are zero, namely $R'=R''=\cdots=0$ in Eqs. (42) and (43), and hence $R\phi$ in Eq. (44) does not have higher terms. Therefore, the response has only the first harmonic in Eq. (14) in the case of R_0. On the other hand, for R depending on heating rate, since $R'\neq 0$ in Eqs. (42) and (43), the kinetic model predicts nonlinear response and higher harmonics. Experimentally, we have already recognized that the modulated heat flow has higher harmonics in the melting range [16–18]. The kinetic modeling presented here is consistent with the experimental results in this sense.

6. Conclusion

The response of the melting kinetics presented here shows a frequency dependence well fitted with the analytical solutions in both cases of Gaussian distribution and uniform distribution of the melting points if the change in the distribution is small enough and the condition is of heating only. The characteristic time required for the melting of a fraction is dependent on heating rate due to the superheating dependence of the melting-rate coefficient. It is pointed out that the nonlinear response of the kinetics is an essential feature of the melting kinetics depending on the degree of superheating. Though we recognize that the raw data of T-MDSC includes the response of DSC apparatus (heat transfer coefficient, heat capacity of sample stage, etc.) and the calibration to the magnitude and phase angle is important for the melting region,[2] the present work clearly demonstrated that the response of the melting kinetics can explain the basic feature of the apparent heat capacity obtained with T-MDSC in the melting region of polymer crystals. Taking into account the response of the DSC apparatus, an extension of the simulation method is now under progress. The significance of the calibration will be clarified by this approach.

Acknowledgements

This work was partly supported by a Grant-in-Aid for Scientific Research from the Ministry of Education, Science and Culture of Japan.

References

[1] P.S. Gill, S.R. Sauerbrunn, M. Reading, J. Therm. Anal. 40 (1993) 931.
[2] M. Reading, D. Elliott, V.L. Hill, J. Therm. Anal. 40 (1993) 949.
[3] M. Reading, A. Luget, R. Wilson, Thermochim. Acta 238 (1994) 295.
[4] B. Wunderlich, Y. Jin, A. Boller, Thermochim. Acta 238 (1994) 277.
[5] A. Boller, Y. Jin, B. Wunderlich, J. Therm. Anal. 42 (1994) 307.
[6] I. Hatta, Jpn. J. Appl. Phys. 33 (1994) L686.
[7] N.O. Birge, S.R. Nagel, Phys. Rev. Lett. 54 (1985) 2674.
[8] A. Hensel, J. Dobbertin, J.E.K. Schawe, A. Boller, C. Schick, J. Therm. Anal. 46 (1996) 935.
[9] A. Toda, C. Tomita, M. Hikosaka, Prog. Theoret. Phys. Suppl. 126 (1997) 103.
[10] J.E.K. Schawe, G.W.H. Höhne, J. Therm. Anal. 46 (1996) 893.
[11] A. Toda, T. Oda, M. Hikosaka, Y. Saruyama, Polymer 38 (1997) 231.

[2] The importance of the calibration in the melting region has been pointed out independently [21].

[12] A. Toda, T. Oda, M. Hikosaka, Y. Saruyama, Thermochim. Acta 293 (1997) 47.
[13] A. Toda, C. Tomita, M. Hikosaka, Y. Saruyama, Polymer 38 (1997) 2849.
[14] A. Toda, C. Tomita, M. Hikosaka, Y. Saruyama, Polymer 39 (1998) 1439.
[15] J.E.K. Schawe, Thermochim. Acta 271 (1996) 127.
[16] A. Toda, C. Tomita, M. Hikosaka, Y. Saruyama, Polymer 39 (1998) 5093.
[17] A. Toda, C. Tomita, M. Hikosaka, Y. Saruyama, Thermochim. Acta 324 (1998) 95.
[18] A. Toda, C. Tomita, M. Hikosaka, J. Therm. Anal. 54 (1998) 623.
[19] J.E.K. Schawe, Thermochim. Acta 260 (1995) 1.
[20] B. Wunderlich, Macromolecular Physics, vol. 3, Chapters 8 and 9, Academic Press, New York, 1976.
[21] M. Reading, J.E.K. Schawe, M. Merzlyakov, C. Schick, A. Toda, The Fifth Lähnwitz Seminar on Calorimetry, Kühlungsborn, Germany, 7–12 June 1998.